

Interfacial superconductivity induced by single-quintuple-layer Bi_2Te_3 on top of FeTe forming van-der-Waals heterostructure

Hailang Qin,^{1,2} Bin Guo,¹ Linjing Wang,¹ Meng Zhang,¹ Bochao Xu,¹ Kaige Shi,¹ Tianluo Pan,¹ Liang Zhou,¹ Yang Qiu,³ Bin Xi,⁴ Iam Keong Sou,⁵ Dapeng Yu,¹ Wei-Qiang Chen,¹ Hongtao He,^{1,*} Fei Ye,^{1,†} Jia-Wei Mei,^{1,‡} and Gan Wang^{1,2,§}

¹*Shenzhen Institute for Quantum Science and Engineering, and Department of Physics, Southern University of Science and Technology, Shenzhen 518055, China*

²*Shenzhen Key Laboratory of Quantum Science and Engineering, Shenzhen 518055, China*

³*Materials Characterization and Preparation Center, Southern University of Science and Technology, Shenzhen 518055, China*

⁴*College of Physics Science and Technology, Yangzhou University, Yangzhou 225002, China*

⁵*Department of Physics, the Hong Kong University of Science and Technology, Hong Kong, China*

(Dated: March 18, 2019)

We report the first clear observation of interfacial superconductivity on top of FeTe (FT) covered by one quintuple-layer Bi_2Te_3 (BT) forming van-der-Waals heterojunction. Both transport and scanning tunneling spectroscopy measurements confirm the occurrence of superconductivity at a transition temperature $T_c = 13$ K, when a single-quintuple-layer BT is deposited on the non-superconducting FT surface. The superconductivity gap decays exponentially with the thickness of BT, suggesting it occurs at the BT-FT interface and the proximity length is above 5 - 6 nm. We also measure the work function's dependence on the thickness of BT, implying a charge transfer may occur at the BT/FT interface to introduce hole doping into the FT layer, which may serve as a possible candidate for the superconducting mechanism. Our BT/FT heterojunction provides a clean system to study the unconventional interfacial superconductivity.

The interfacial superconductivity has been of great interest [1–7], since it may help to resolve the mystery of high temperature superconductors with layered structures and to search for the topological superconductors [8–10]. There are several mechanisms proposed for the interfacial superconductivity, including edge misfit dislocation defect [2, 11], electric field gating [3, 4] as well as chemical doping (e.g. charge transfer) [5, 6]. In order to pin down the superconducting mechanism unambiguously, the high quality sample with atomic abruptness at the interfaces is required. In the past decade, van der Waals (vdW) epitaxy turns out to be an effective way to grow two-dimensional interfacial superconductors [8–10, 12], where the interface is usually of high quality even against the large lattice mismatch since the interfacial interaction at the heterojunctions is of vdW type[13].

$\text{Bi}_2\text{Te}_3/\text{Fe}_{1+x}\text{Te}$ is one of the first realized van der Waals heterostructures which hosts an interfacial superconductivity between two non-superconductors Bi_2Te_3 and Fe_{1+x}Te [8, 9], where Fe_{1+x}Te may have an unusual mechanism for superconductivity and magnetic order of '11' group iron based superconductors [14, 15]. A transport study showed that an optimal superconductivity ($T_c = 11.5$ K) only can be developed when the Bi_2Te_3 layer reaches a thickness of 5 quintuple-layer (QL) while single QL $\text{Bi}_2\text{Te}_3/\text{Fe}_{1+x}\text{Te}$ only possesses a low T_c around 2 K, indicating Bi_2Te_3 thickness may be crucial for the formation of superconductivity [9]. In the past years, great efforts have been devoted to studying the intriguing superconductivity of $\text{Bi}_2\text{Te}_3/\text{Fe}_{1+x}\text{Te}$ [16–20]. For instance, Gu et al. reported a scanning tunneling mi-

croscopy (STM) study on the Bi_2Te_3 grown on Fe_{1+x}Te , however, the energy gap of superconductivity didn't appear even Bi_2Te_3 is thicker than 6 QLs, instead a merging of Dirac electrons and the correlation effect was revealed in the scanning tunneling spectroscopy (STS), implying the thickness of Bi_2Te_3 is not the exclusive cause of superconductivity [16]. In 2017, Manna et al. studied a reverse structure, FeTe grown on bulk Bi_2Te_3 crystal, and probed an energy gap of superconductivity co-existing with bicollinear antiferromagnetic (AFM) order [18], however, the gap revealed T_c is lower than 6 K, inconsistent with the previous transport transport results [9], as in their sample the Bi_2Te_3 layer is thicker than the optimal 5 QLs. Obviously, the mechanism for $\text{Bi}_2\text{Te}_3/\text{Fe}_{1+x}\text{Te}$ superconductivity is still a matter of debate, including the location of superconductivity and the possible driving factors, nevertheless, the revealed correlation effect and unusual AFM order made the system very attractive for studying the unusual mechanism for iron based superconductors.

In this work, we report the STM study of high quality $\text{Bi}_2\text{Te}_3/\text{FeTe}$ interface grown on $\text{SrTiO}_3(001)$ (STO) substrates. Remarkably, we found that an interfacial superconductivity immediately appeared once one QL Bi_2Te_3 patched the FeTe surface, with a high T_c around 13 K confirmed by STS and transport study simultaneously. Furthermore, we present the first superconducting energy gap evolution of $\text{Bi}_2\text{Te}_3/\text{FeTe}$ interface, implying that the superconductivity on the thicker Bi_2Te_3 (2-5QL) layer is proximity-induced and the superconductivity is essentially located at the Bi_2Te_3 - FeTe interface (includ-

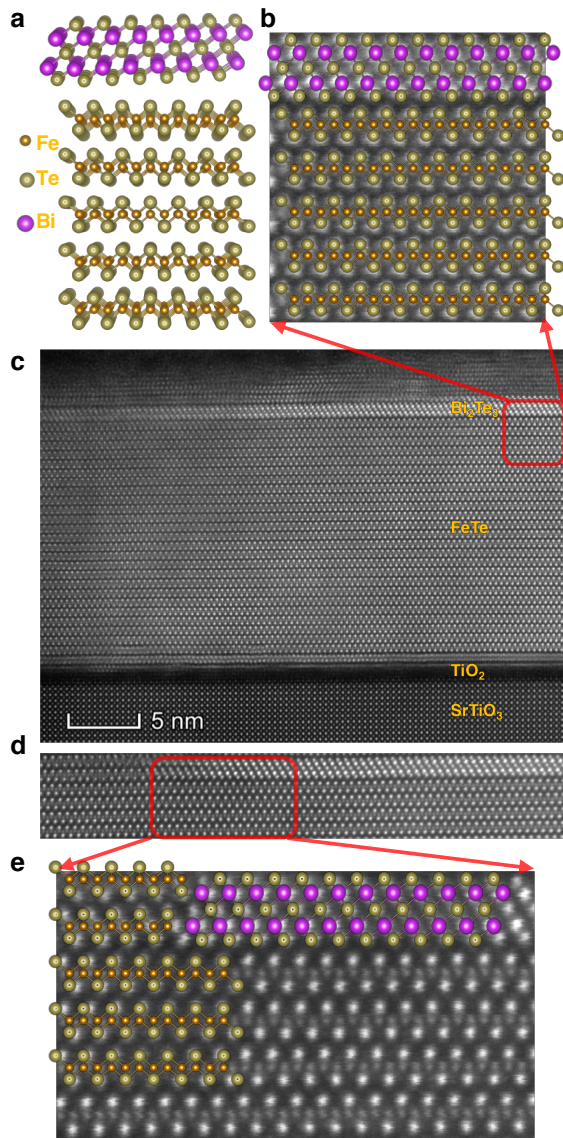


FIG. 1. (a) A schematic illustration for 1 QL Bi₂Te₃ grown on FeTe. (b) A lattice comparison for a Bi₂Te₃/FeTe interface. (c) A HRSTEM image containing a Bi₂Te₃ (1 QL), a FeTe(20nm) thin film and a STO substrate simultaneously. (d) A HRTEM image of a lateral heterojunction formed by a Bi₂Te₃ quintuple layer and a FeTe atomic step. (e) A lattice comparison for the lateral heterojunction and its nearby FeTe

ing the cases of within one QL of Bi₂Te₃ and within one monolayer of FeTe). Via a deliberate measurement of work function change with Bi₂Te₃ thickness, we also found that the superconductivity is likely induced by a hole-doping effect on FeTe due to the band mis-alignment between Bi₂Te₃ and FeTe. We believe that our findings will contribute the key facts for resolving the unconventional interfacial superconductivity in the Bi₂Te₃/FeTe interface.

The samples were grown on single crystal 0.7% wt Nb-doped STO(001) substrates. The STO substrate was

first gradually heated to about 950°C by electron-beam heating and annealed at this temperature for about 30 minutes. The substrate was then transferred *in-situ* to an adjacent Createc molecular beam epitaxy (MBE) system for sample growth. The FeTe thin films were grown in the MBE chamber by co-evaporation of high purity Fe (99.995%) and Te (99.999%) onto the substrate held at around 300 °C, with a Te rich flux ratio to ensure the stoichiometry. The thickness of FeTe layer is around 20 nm. The Bi₂Te₃ thin films were then grown by evaporating Bi₂Te₃ compound source at the substrate temperature of about 225 °C, with a growth rate around 2.5 Å/min for ensuring the precise QL control. Reflective high energy electron diffraction (RHEED) patterns (supplementary 1) kept streaky during the entire growth, indicating a layer-by-layer growth mode dominating the epitaxy. The samples were then transferred *in-situ* to a SPECS Joule-Thomson (JT) STM system. The base pressure in the MBE chamber and STO chamber was about 3×10^{-10} mbar and 5×10^{-10} mbar, respectively. The STM measurements were performed at 1.1 K (unless otherwise specified) with etched tungsten tips, which were sputtered with an Ar⁺ ion sputter gun and tested on a reference Au(111). A high resolution scanning transmission electron microscopy (HRSTEM) was employed for a cross-sectional characterization on a Bi₂Te₃(1QL)/FeTe(20nm) bilayer sample cut by a focus ion beam technique. Transport measurements were carried out with a standard four-point probe method using a commercial Quantum Design physical property measurement (PPMS) system. The ultraviolet photoemission spectroscopy (UPS) measurements were carried out using a SPECS PHOIBOS 150 hemispherical energy analyzer and a light source from a helium discharge lamp (He I, photon energy 21.218 eV).

Fig. 1 (a) suggests a cross-sectional schematic illustration of 1 QL Bi₂Te₃ grown on FeTe, well matching the lattice of the red square indicated region (Fig. 1 (b)) shown in the HRSTEM Fig. 1 (c), evidencing a sharp vdW interface without lattice distortion or inter-diffusion. Furthermore, a typical lateral Bi₂Te₃-FeTe heterojunction near a FeTe atomic step is imaged in Fig. 1 (d) and 1 (e), demonstrating a step-flow epitaxy. It is worth mentioning that no interstitial Fe atoms were detected by a careful examining the FeTe lattice shown in Fig. 1 (c). Combining with the 1:1 ratio of Fe/Te revealed by chemical analysis (see supplementary materials), we assert that the FeTe film is of strict stoichiometry, similar as previous reported stoichiometric FeTe thin films grown by MBE with Te rich flux [21].

The STM studies were carried out on more than 20 samples and the results are repeatable and consistent. Fig. 2 (a) is a typical topographic image after growth of about 1~2 QL of Bi₂Te₃, inside which we acquire atomic-resolution images of exposed FeTe surface and 1 QL Bi₂Te₃ surface shown in Fig. 2 (c) and (d), respec-

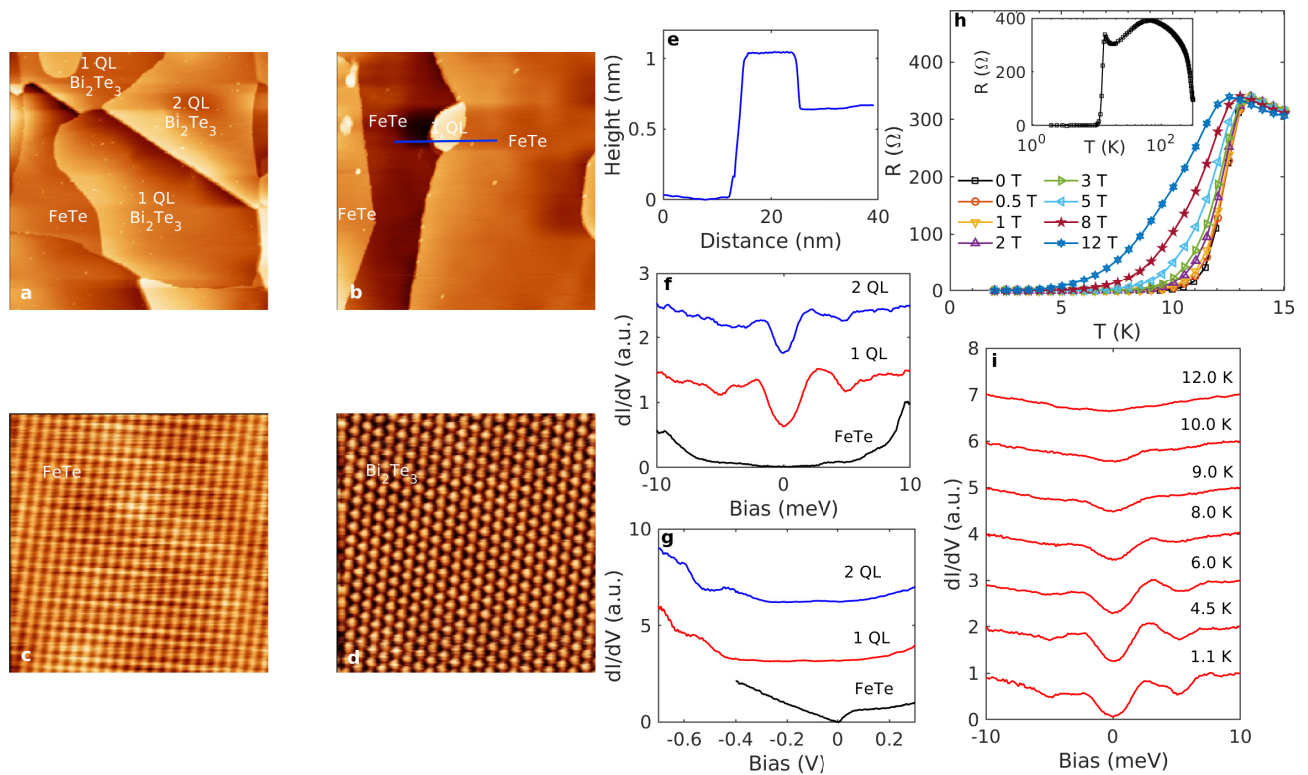


FIG. 2. (a) A STM topographic image of an area containing exposed FeTe, 1 QL and 2 QLS of Bi_2Te_3 (size: $220 \times 220 \text{ nm}^2$, $V_{\text{Bias}} = 2.0 \text{ V}$, $I_{\text{Tunnel}} = 50 \text{ pA}$, color scale: 1.57 nm). (b) A STM topographic image showing how Bi_2Te_3 typically grows on FeTe films (size: $100 \times 100 \text{ nm}^2$, $V_{\text{Bias}} = 1.8 \text{ V}$, $I_{\text{Tunnel}} = 50 \text{ pA}$, color scale: 1.24 nm). (c) An atomic resolution image of the exposed FeTe surface (size: $8 \times 8 \text{ nm}^2$, $V_{\text{Bias}} = -10 \text{ mV}$, $I_{\text{Tunnel}} = 200 \text{ pA}$, color scale: 0.03 nm). (d) An atomic resolution image of the 1 QL Bi_2Te_3 surface (size: $8 \times 8 \text{ nm}^2$, $V_{\text{Bias}} = 6.5 \text{ mV}$, $I_{\text{Tunnel}} = 400 \text{ pA}$, color scale: 0.03 nm). (e) A line profile corresponding to the blue line in (b). (f). Representative dI/dV spectra acquired on the FeTe surface, 1 QL Bi_2Te_3 , and 2 QL Bi_2Te_3 terraces, respectively (set point: $V_{\text{Bias}} = 10 \text{ mV}$, $I_{\text{Tunnel}} = 50 \text{ pA}$). (g) Representative dI/dV spectra in a wider bias range acquired on the FeTe surface, 1 QL Bi_2Te_3 , and 2 QL Bi_2Te_3 terraces, respectively (set point: $V_{\text{Bias}} = 0.3 \text{ V}$, $I_{\text{Tunnel}} = 50 \text{ pA}$). (h). Temperature dependent resistance R - T curve of a sample of 1nm Bi_2Te_3 /40 nm FeTe/STO under different magnetic fields perpendicular to the interface. The inset in (h) shows the R - T curve of the same sample in a wider temperature range without applying magnetic field. (i) Temperature dependent dI/dV spectra acquired on the 1 QL Bi_2Te_3 (set point: $V_{\text{Bias}} = 10 \text{ mV}$, $I_{\text{Tunnel}} = 50 \text{ pA}$). The texts in the all the STM images indicate the respective areas identified. Measured temperature is 1.1 K.

tively, representing a perfect lattice without any adatoms and vacancies being observed. The growth time for the sample in Fig. 2(b) was extremely short to observe the growth behavior, showing a nucleation of Bi_2Te_3 takes place on the atomic step of FeTe, consistent with cross-sectional HRSTEM results shown in Fig. 1. Fig. 2 (e) is the line profile corresponding to the blue line in Fig. 2 (b). The step height of about 0.6 nm and 1.0 nm correspond to one unit cell of FeTe and 1 QL layer of Bi_2Te_3 , respectively. Representative dI/dV spectra in a narrow bias range acquired on the FeTe, 1 QL Bi_2Te_3 , and 2 QL Bi_2Te_3 terraces are shown in Fig. 2 (f). dI/dV measures the local DOS near the Fermi level. The spectra acquired on the 1 QL Bi_2Te_3 terrace show two clear coherent superconducting peaks around 2.5 meV. This is in clear contrast to the spectrum acquired on the FeTe surface, which shows no coherent peaks, but a valley shape spec-

trum with a flat bottom. On the 2 QL Bi_2Te_3 , the spectrum also exhibits two coherent superconducting peaks; however, the peaks are smaller at around 1.8 meV. The spectra on each terrace also vary little, indicating a good uniformity of the superconductivity. The temperature dependent dI/dV spectra on the 1 QL Bi_2Te_3 surface are shown in Fig. 2 (i), while the results on the 2 QL are in the Supplementary Materials [22]. While no significant change in the intensity of the coherence peak for the spectra is observed for temperature below 6 K, there is a significant decrease in the peak intensity at temperatures above 6 K. The gap magnitude is discernible up to about 10 K. At 12 K, there is no clear gap observed, consistent with followed transport revealed T_c . Typical dI/dV spectra in a wider bias range obtained in the FeTe, 1 QL Bi_2Te_3 , and 2 QL Bi_2Te_3 surfaces are plotted in Fig. 2 (g). According to the dI/dV spectrum Bi_2Te_3 film

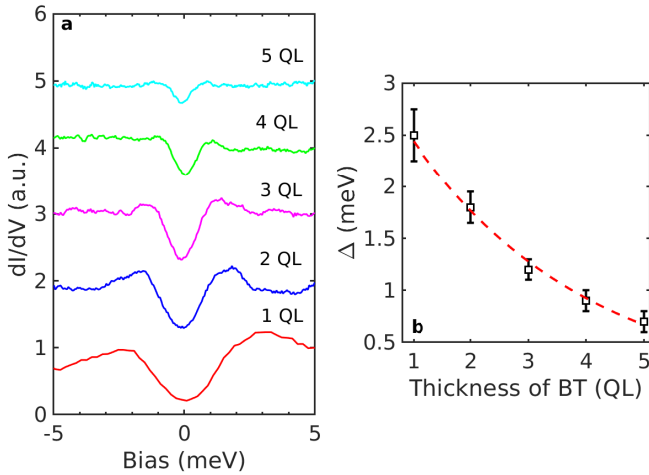


FIG. 3. (a) Representative dI/dV spectra acquired on 1 QL, 2 QL, 3 QL, 4 QL, and 5 QL Bi₂Te₃ surfaces, respectively. Spectra were shifted vertically for clarity. (b) Gap magnitude versus the Bi₂Te₃ thickness.

of 1 QL, there is discernibly weak and nearly constant density of states from 0 eV (Fermi level) to -0.43 eV. Below about -0.43 eV, the density of states start to rise rapidly with a kink at about -0.55 eV. On the Bi₂Te₃ film of 2 QL, there are two kinks around 0.08 eV and -0.44 eV, likely corresponding to the conduction band minimum (CBM) and valence band maximum (VBM), respectively. Comparing with the dI/dV spectrum on the thick Bi₂Te₃ film [22], it indicates that the 1 QL Bi₂Te₃ film and 2 QL Bi₂Te₃ film are both more n-type doped. While this is qualitatively consistent with what is observed by Xu et al. [23], the Fermi level shifts on the 1 QL and 2 QL Bi₂Te₃ are more significant, indicating the electron doping effect from the FeTe film likely plays an important role.

The temperature dependent in-plane resistance (R - T curve) of a Bi₂Te₃/FeTe/STO device with an average Bi₂Te₃ thickness of around 1 QL is shown in Fig. 2 (h). In the zero field (the inset in Fig. 2 (h)), a broad transition at about 65 K is observed, likely related to the magnetic and/or structural transition of FeTe films [14, 24–29]. The RT curve shows a superconducting transition with an onset temperature of $T_c^{\text{onset}} = 13$ K and zero resistance temperature of $T_c^0 = 7.5$ K. Before T_c^{onset} , there is a upturn in R - T curve with decreasing temperature. The magnetic field (applied perpendicular to the sample interface) suppresses the superconductivity, and 12 T field is far away to completely kill the superconductivity, indicating a very high critical field, which is a characteristic feature of FeTe based superconductors [30].

The dI/dV spectra were acquired on samples with thicker Bi₂Te₃ films up to about 5-6 QL and are all shown in Fig. 3 (a). As can be seen, all of these spectra exhibit two coherent peaks, whereas the gap magnitude decreases

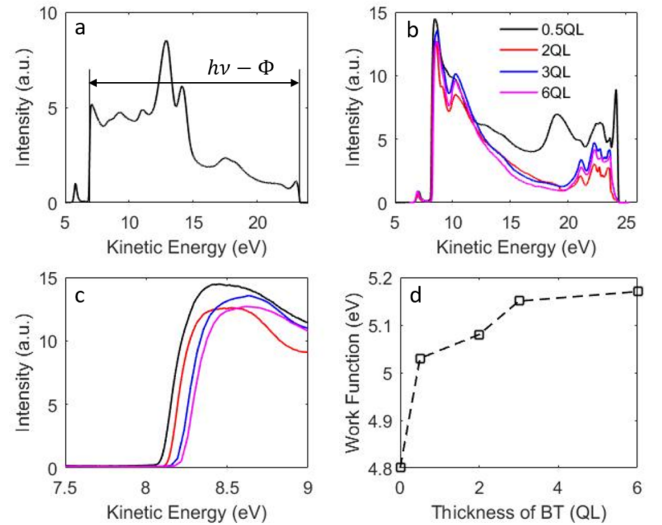


FIG. 4. (a). UPS spectrum of FeTe film taken with -2 V bias applied to the sample. (b). UPS spectra of Bi₂Te₃/FeTe samples taken with -3 V bias with average Bi₂Te₃ thickness of 0.5 QL (black), 2 QL (red), 3 QL (blue), and 6 QL (magenta), respectively. (c). Zoom-in view of (b) around the inelastic cutoff region at lower kinetic energy. (d) Extracted work function from UPS spectra in (a) and (b).

with increasing Bi₂Te₃ thickness. The gap magnitude Δ of the spectra is plotted in Fig. 3 (b) with respect to the number of QLs of Bi₂Te₃. The Δ shows an exponential decay with a relationship of $\Delta = 3.376e^{-\frac{N}{3.087}}$ (in unit of meV, N is the number of QLs of Bi₂Te₃) as obtained from the fitting, consistent with the characteristic of proximity-induced superconductivity [12], from which we can infer that the superconductivity is not enhanced in any way when the Bi₂Te₃ is 2 QLs or more than that when the Bi₂Te₃ is only 1 QL; instead, the superconductivity locates in the 1 QL Bi₂Te₃/FeTe interface, and becomes weaker on the Bi₂Te₃ surface due to the proximity effect.

To further unveil the charge transfer mechanism between Bi₂Te₃ and FeTe, we also *in-situ* measured the work function of the FeTe film before and after the growing of Bi₂Te₃ film with average thickness of 0.5 QL, 2 QL, 3 QL, and 6 QL, respectively using UPS at 15 K. The UPS result of FeTe film is shown in Fig. 4 (a). A voltage -2 V was applied between the sample and the spectrometer so that the photoelectrons were accelerated and then the low energy inelastic electrons could be distinguished from secondary electrons generated in the spectrometer by impact [31], which can be seen in Fig. 4 (a) as a small peak near 5.5 eV. The work function is calculated with the formula $\Phi = h\nu - \Delta E$, where $h\nu$ is the photon energy and ΔE is the spectrum width, the distance between the low energy cutoff and the Fermi edge as shown in Fig. 4 (a). Then we measured the photoemission spectrums of Bi₂Te₃ covered- FeTe with increasing thickness

of Bi_2Te_3 and the results are shown in Fig. 4 (b). The zoom-in view of the low kinetic energy region of Fig. 4 (b) is shown in Fig. 4 (c), depicting that the inelastic edge offsets to the high kinetic energy region as the thickness of Bi_2Te_3 being increased, while the fermi edge in the high energy end is pinned in all the spectrums as they are determined by the accelerating voltage(- 3 V) solely. The extracted work functions are shown in Fig. 4 (d). As can be seen, the work function of FeTe film is about 4.80 eV. With the growth of Bi_2Te_3 , the work function increases gradually, and starts to saturate when the Bi_2Te_3 thickness reaches about 3 QL. This result clearly suggests that there is a doping effect when the Bi_2Te_3 film is deposited onto the FeTe film, i.e., FeTe is hole-doped and Bi_2Te_3 film is electron-doped, qualitatively consistent the STS revealed charge transfer in Fig. 2 (g).

In the heterostructure of $\text{Bi}_2\text{Te}_3/\text{FeTe}$ in our study, neither Bi_2Te_3 or FeTe is superconducting. Upon doping, Bi_2Te_3 is only superconducting with a maximum reported transition temperature of 5.5 K [32]. On the other hand, FeTe is superconducting upon doping with either oxygen [30] or selenium [33] with a transition temperature of about 14 K, which is surprisingly close to the transition temperature in our study. Our work function measurements clearly show that there is a hole doping effect on the FeTe layer in the heterostructure. Therefore, it is plausible that the single FeTe layer become superconductivity due to the loss of electrons induced by Bi_2Te_3 covering, leading to the interface superconductivity observed in our study. While it still remains a challenge on how this doping leads to the observed superconductivity, our results provide more insights for future theoretic work to understand this doping induced change on electronic and magnetic properties of a single FeTe layer, which may also shed light on resolving the mystery of iron based superconductivity.

In conclusion, the superconductivity of $\text{Bi}_2\text{Te}_3/\text{FeTe}$ system is studied by using the low temperature scanning tunneling microscopy. It is found that the superconductivity in the $\text{Bi}_2\text{Te}_3/\text{FeTe}$ system can be induced by only one QL of Bi_2Te_3 , which is also confirmed by the transport measurements. Scanning tunneling spectroscopy further shows that the superconducting gap decays exponentially with the increasing Bi_2Te_3 thickness, implying the superconductivity in Bi_2Te_3 bulk is actually proximity-induced by the interface. Our results provide unambiguous evidence that the superconductivity in the $\text{Bi}_2\text{Te}_3/\text{FeTe}$ system is located around the $\text{Bi}_2\text{Te}_3/\text{FeTe}$ interface. As for the superconducting mechanism, it is found that the doping of FeTe may be possible to generate superconductivity in the $\text{Bi}_2\text{Te}_3/\text{FeTe}$ vdW heterojunctions.

We thanks H. H. Wen, L. Yu and P. A. Marchetti for discussions. This work was supported by the National Natural Science Foundation of China (NO. 61734008 and 11774143), the National Key Research and De-

velopment Program of China (No. 2018YFA0307100, No. 2016YFA0301703), the Natural Science Foundation of Guangdong Province (No. 2015A030313840, No. 2017A030313033), the State Key Laboratory of Low-Dimensional Quantum Physics (No. KF201602), Technology and Innovation Commission of Shenzhen Municipality (ZDSYS20170303165926217 and JCYJ20170412152334605). J.W.M was partially supported by the program for Guangdong Introducing Innovative and Entrepreneurial Teams (No. 2017ZT07C062).

* heht@sustech.edu.cn

† yef@sustech.edu.cn

‡ meijw@sustech.edu.cn

§ wangg@sustech.edu.cn

- [1] V. L. Ginzburg, "On surface superconductivity," *Physics Letters* **13**, 101–102 (1964).
- [2] D. L. Miller, Myron Strongin, O. F. Kammerer, and B. G. Streetman, "Superconductivity at the surface of pbte," *Phys. Rev. B* **8**, 4416–4419 (1973).
- [3] C. H. Ahn, S. Gariglio, P. Paruch, T. Tybell, L. Antognazza, and J.-M. Triscone, "Electrostatic modulation of superconductivity in ultrathin $\text{gdb}_2\text{cu}_3\text{o}_7\text{-x}$ films," *Science* **284**, 1152–1155 (1999).
- [4] C. H. Ahn, J.-M. Triscone, and J. Mannhart, "Electric field effect in correlated oxide systems," *Nature* **424**, 1015 (2003).
- [5] N. Reyren, S. Thiel, A. D. Caviglia, L. Fitting Kourkoutis, G. Hammerl, C. Richter, C. W. Schneider, T. Kopp, A.-S. Rüetschi, D. Jaccard, M. Gabay, D. A. Muller, J.-M. Triscone, and J. Mannhart, "Superconducting interfaces between insulating oxides," *Science* **317**, 1196–1199 (2007).
- [6] A. Gozar, G. Logvenov, L. Fitting Kourkoutis, A. T. Bollinger, L. A. Giannuzzi, D. A. Muller, and I. Bozovic, "High-temperature interface superconductivity between metallic and insulating copper oxides," *Nature* **455**, 782 (2008).
- [7] Juan Pereiro, Alexander Petrovic, Christos Panagopoulos, and Ivan Božović, "Interface superconductivity: History, development and prospects," arXiv preprint arXiv:1111.4194 (2011).
- [8] Gan Wang, Qing Lin He, Hong-Tao He, Hong-Chao Liu, Mingquan He, Jian-Nong Wang, Rolf Lortz, George Ke Lun Wong, and Iam Keong Sou, "Formation mechanism of superconducting $\text{fe}_1\text{+xte}/\text{bi}_2\text{te}_3$ bilayer synthesized via interfacial chemical reactions," *Crystal Growth & Design* **14**, 3370–3374 (2014).
- [9] Qing Lin He, Hongchao Liu, Mingquan He, Ying Hoi Lai, Hongtao He, Gan Wang, Kam Tuen Law, Rolf Lortz, Jiannong Wang, and Iam Keong Sou, "Two-dimensional superconductivity at the interface of a $\text{Bi}_2\text{Te}_3/\text{FeTe}$ heterostructure," *Nature Communications* **5**, 4247 (2014).
- [10] Yi-Min Zhang, Jia-Qi Fan, Wen-Lin Wang, Ding Zhang, Lili Wang, Wei Li, Ke He, Can-Li Song, Xu-Cun Ma, and Qi-Kun Xue, "Observation of interface superconductivity in a $\text{snse}_2/\text{epitaxial graphene van der waals heterostructure}$," *Phys. Rev. B* **98**, 220508 (2018).
- [11] Nina Ya. Fogel, V. G. Cherkasova, A. S. Pokhila, A. Yu.

- Sipatov, and A. I. Fedorenko, “Superconductivity in the novel semiconducting superlattices,” *Czechoslovak Journal of Physics* **46**, 727–728 (1996).
- [12] Jin-Peng Xu, Canhua Liu, Mei-Xiao Wang, Jianfeng Ge, Zhi-Long Liu, Xiaojun Yang, Yan Chen, Ying Liu, Zhu-An Xu, Chun-Lei Gao, Dong Qian, Fu-Chun Zhang, and Jin-Feng Jia, “Artificial topological superconductor by the proximity effect,” *Phys. Rev. Lett.* **112**, 217001 (2014).
- [13] Atsushi Koma, “Van der waals epitaxya new epitaxial growth method for a highly lattice-mismatched system,” *Thin Solid Films* **216**, 72 – 76 (1992).
- [14] Wei Bao, Y. Qiu, Q. Huang, M. A. Green, P. Zajdel, M. R. Fitzsimmons, M. Zhernenkov, S. Chang, Minghu Fang, B. Qian, E. K. Vehstedt, Jinhu Yang, H. M. Pham, L. Spinu, and Z. Q. Mao, “Tunable ($\delta\pi$, $\delta\pi$)-type antiferromagnetic order in α -fe(te,se) superconductors,” *Phys. Rev. Lett.* **102**, 247001 (2009).
- [15] Y. Xia, D. Qian, L. Wray, D. Hsieh, G. F. Chen, J. L. Luo, N. L. Wang, and M. Z. Hasan, “Fermi surface topology and low-lying quasiparticle dynamics of parent $fe_{1+x}Te/Se$ superconductor,” *Phys. Rev. Lett.* **103**, 037002 (2009).
- [16] Guan Du, Zengyi Du, Xiong Yang, Enyu Wang, De-long Fang, Huan Yang, and Hai-Hu Wen, “Merging dirac electrons and correlation effect in the heterostructured $bi_2te_3/fe_{1+x}te$,” *arXiv preprint arXiv:1509.07424* (2015).
- [17] M. N. Kunchur, C. L. Dean, N. Shayesteh Moghadam, J. M. Knight, Q. L. He, H. Liu, J. Wang, R. Lortz, I. K. Sou, and A. Gurevich, “Current-induced depairing in the $bi_2te_3/FeTe$ interfacial superconductor,” *Phys. Rev. B* **92**, 094502 (2015).
- [18] Sujit Manna, Anand Kamalpure, Lasse Cornils, Torben Hänke, Ellen Marie Jensen Hedegaard, Martin Bremholm, Bo Brummerstedt Iversen, Ph Hofmann, Jens Wiebe, and Roland Wiesendanger, “Interfacial superconductivity in a bi-collinear antiferromagnetically ordered fete monolayer on a topological insulator,” *Nature communications* **8**, 14074 (2017).
- [19] Fabian Arnold, Jonas Warmuth, Matteo Michiardi, Jan Fikek, Marco Bianchi, Jin Hu, Zhiqiang Mao, Jill Miwa, Udai Raj Singh, Martin Bremholm, Roland Wiesendanger, Jan Honolka, Tim Wehling, Jens Wiebe, and Philip Hofmann, “Electronic structure of $fe_{1.08}te$ bulk crystals and epitaxial fete thin films on bi_2te_3 ,” *Journal of Physics: Condensed Matter* **30**, 065502 (2018).
- [20] Udai Raj Singh, Jonas Warmuth, Anand Kamalpure, Lasse Cornils, Martin Bremholm, Philip Hofmann, Jens Wiebe, and Roland Wiesendanger, “Enhanced spin-ordering temperature in ultrathin fete films grown on a topological insulator,” *Phys. Rev. B* **97**, 144513 (2018).
- [21] Wei Li, Wei-Guo Yin, Lili Wang, Ke He, Xucun Ma, Qi-Kun Xue, and Xi Chen, “Charge ordering in stoichiometric fete: Scanning tunneling microscopy and spectroscopy,” *Phys. Rev. B* **93**, 041101 (2016).
- [22] Hello world.
- [23] Jin-Peng Xu, Mei-Xiao Wang, Zhi Long Liu, Jian-Feng Ge, Xiaojun Yang, Canhua Liu, Zhu An Xu, Dandan Guan, Chun Lei Gao, Dong Qian, Ying Liu, Qiang-Hua Wang, Fu-Chun Zhang, Qi-Kun Xue, and Jin-Feng Jia, “Experimental detection of a majorana mode in the core of a magnetic vortex inside a topological insulator-superconductor $bi_2te_3/nbse_2$ heterostructure,” *Phys. Rev. Lett.* **114**, 017001 (2015).
- [24] Shiliang Li, Clarina de la Cruz, Q. Huang, Y. Chen, J. W. Lynn, Jiangping Hu, Yi-Lin Huang, Fong-Chi Hsu, Kuo-Wei Yeh, Maw-Kuen Wu, and Pengcheng Dai, “First-order magnetic and structural phase transitions in $fe_{1+y}se_xte_{1-x}$,” *Phys. Rev. B* **79**, 054503 (2009).
- [25] S. Röbller, Dona Cherian, W. Lorenz, M. Doerr, C. Koz, C. Curfs, Yu. Prots, U. K. Röbller, U. Schwarz, Suja Elizabeth, and S. Wirth, “First-order structural transition in the magnetically ordered phase of $fe_{1.13}te$,” *Phys. Rev. B* **84**, 174506 (2011).
- [26] E. E. Rodriguez, C. Stock, P. Zajdel, K. L. Krycka, C. F. Majkrzak, P. Zavalij, and M. A. Green, “Magnetic-crystallographic phase diagram of the superconducting parent compound $fe_{1+x}te$,” *Phys. Rev. B* **84**, 064403 (2011).
- [27] Yoshikazu Mizuguchi, Kentaro Hamada, Kazuki Goto, Hiroshi Takatsu, Hiroaki Kadowaki, and Osuke Miura, “Evolution of two-step structural phase transition in fe_{1+dte} detected by low-temperature x-ray diffraction,” *Solid State Communications* **152**, 1047 – 1051 (2012).
- [28] I. A. Zaliznyak, Z. J. Xu, J. S. Wen, J. M. Tranquada, G. D. Gu, V. Solovyov, V. N. Glazkov, A. I. Zheludev, V. O. Garlea, and M. B. Stone, “Continuous magnetic and structural phase transitions in $fe_{1+y}te$,” *Phys. Rev. B* **85**, 085105 (2012).
- [29] Cevriye Koz, Sahana Röbller, Alexander A. Tsirlin, Steffen Wirth, and Ulrich Schwarz, “Low-temperature phase diagram of $fe_{1+y}te$ studied using x-ray diffraction,” *Phys. Rev. B* **88**, 094509 (2013).
- [30] Weidong Si, Qing Jie, Lijun Wu, Juan Zhou, Genda Gu, P. D. Johnson, and Qiang Li, “Superconductivity in epitaxial thin films of $fe_{1.08}Te : o_x$,” *Phys. Rev. B* **81**, 092506 (2010).
- [31] Rudy Schlaf, “Calibration of photoemission spectra and work function determination,” <http://rsl.eng.usf.edu/Documents/Tutorials/PEScalibration.pdf>.
- [32] Y.S. Hor, J.G. Checkelsky, D. Qu, N.P. Ong, and R.J. Cava, “Superconductivity and non-metallicity induced by doping the topological insulators bi_2se_3 and bi_2te_3 ,” *Journal of Physics and Chemistry of Solids* **72**, 572 – 576 (2011), spectroscopies in Novel Superconductors 2010.
- [33] M. H. Fang, H. M. Pham, B. Qian, T. J. Liu, E. K. Vehstedt, Y. Liu, L. Spinu, and Z. Q. Mao, “Superconductivity close to magnetic instability in $Fe(Se_{1-x}Te_x)_{0.82}$,” *Phys. Rev. B* **78**, 224503 (2008).